

Two-dimensional Wigner lattice in a magnetic field and in the presence of a random array of pinning centers

A. G. Eguluz and A. A. Maradudin

Department of Physics, University of California, Irvine, California 92717

R. J. Elliott

Department of Theoretical Physics, University of Oxford, 1 Keble Road, Oxford OX1 3NP, Great Britain

(Received 20 September 1982; revised manuscript received 21 January 1983)

We consider a two-dimensional Wigner lattice in the presence of a static external magnetic field perpendicular to the lattice and a random array of pinning centers. The phonons of the electron lattice are treated in the harmonic approximation, and the random distribution of pinning centers is dealt with in the single-site coherent-potential approximation. We obtain the average phonon Green's function and from it the spectral density for the phonons of the electron lattice. The presence of the random array of pinning centers gives rise to a low-frequency gap in the phonon spectral density. Thus the (two-dimensional) mean-square displacement of an electron about its equilibrium lattice site is finite at finite temperatures. The magnitude of the low-frequency gap decreases as the strength of the magnetic field is increased. For sufficiently high fields the gap disappears, but the phonon spectral density vanishes sufficiently fast as $\omega \rightarrow 0$ that the mean-square displacement remains finite at finite temperatures. We present detailed numerical results for the phonon spectral density and electron mean-square displacement, both at $T=0$ K and at finite temperatures. Our results are analyzed from the point of view of the stability of the lattice to thermal fluctuations. We find that at low temperatures ($T \sim 1$ K) both the pinning centers and the magnetic field considerably enhance the localization of the electrons about their lattice sites, thus enhancing the stability of the lattice. At higher temperatures, the electron mean-square displacement depends very weakly on the strength of the magnetic field, and its value is then determined by the concentration and strength of the pinning centers.

I. INTRODUCTION

At sufficiently low densities and temperatures, an electron gas is expected to crystallize into a Wigner lattice.¹ This is because under such conditions the Coulomb interaction energy dominates the kinetic energy and a correlated state becomes energetically favorable.

At the present time the Wigner crystallization has been observed in the case of electrons at the surface of liquid helium.² Such a two-dimensional (2D) system is a nearly ideal Coulomb system for the study of the crystallization transition because the areal density of the electrons can be varied over several orders of magnitude, and the helium surface is essentially free of traps and scattering centers.

Another 2D system for which the electron areal density can be easily varied is that of electrons in an inversion layer at a semiconductor surface.³ In this case, however, the presence of impurities and crystal defects is a feature of the physical system. This has the consequence that the transition to the crystalline state becomes more difficult to study and, in fact,

has not yet been observed. There are, however, results⁴ suggesting the formation of a magnetic-field-induced Wigner glass in the 2D electron system in a silicon inversion layer at $T > 1.2$ K.

Inherent to any such 2D electron system is the fact that for a perfect infinite 2D crystal at any nonzero temperature, the mean-square displacement (MSD) of an electron about its equilibrium lattice site diverges logarithmically with the linear dimensions of the sample. Thus, in principle, an ideal 2D electron crystal would melt at any nonzero temperature.

It has been proposed many times⁵⁻⁸ that the introduction of a dc magnetic field normal to the plane of the lattice should aid in the formation of the crystalline state. This is because a strong magnetic field will quench the vibrational motion of the electrons except for their rapid cyclotron motion. However, the problem persists that for a perfect 2D lattice in the presence of a magnetic field, the electron MSD diverges at any nonzero temperature. Of course, one can render MSD finite by appealing to the fact that in reality the electron system is finite,

and introducing a small wave-vector cutoff in the integral for the MSD, or by assuming the formation of a polycrystalline 2D lattice.⁸ However, it is of theoretical interest to examine the sample-independent localization properties of a 2D electron lattice. This is the purpose of this work.

We assume that the impurities present at a semiconductor surface in which an inversion layer, and thus a 2D electron crystal, can form, can be modeled by a random distribution of pinning centers that are, however, located at (or directly below) the sites of the 2D Wigner crystal. These pinning centers provide a frame of reference whose existence directly implies the breaking of infinitesimal translational invariance in the plane of the 2D electron crystal, and this yields an electron MSD independent of sample size. Of course, it is expected that in reality the positions of the pinning centers would not exactly coincide with the sites of the Wigner crystal. This, in turn, would give rise to a random static distortion of the lattice. The electrons would then execute vibrations about equilibrium positions defined by the sites of this statically distorted Wigner crystal. Nevertheless, the essential physical features of the model of the pinning centers used in this paper, in which the electrons couple harmonically to *points fixed in space* as well as to each other, would remain in the more realistic model of a statically deformed crystal.

It must be emphasized that in this work we do not address the question of whether for any given system the correlated state that forms as a consequence of the Coulomb interaction is one of short-range order (Wigner crystal) or of long-range order (charge-density wave). We simply assume the existence of the Wigner crystal and consider the question of how the combined effects of a dc magnetic field and a random array of pinning centers affect the localization of the electrons about their equilibrium lattice sites, and hence how they affect the likelihood of Wigner crystallization. The opposite case in which the ground state of the system is described by a charge-density wave whose phase is the only dynamical variable in the problem has been studied by Fukuyama and Lee.⁹

The outline of this paper is as follows. In Sec. II we write down the Hamiltonian for a 2D electron crystal in the presence of both a dc magnetic field normal to the plane of the crystal and a random array of pinning centers. In Sec. III we introduce the phonon Green's function describing the lattice vibrations of the 2D electron crystal. The random scattering potential due to the pinning centers gives rise to a phonon self-energy. The average Green's function and its self-energy are obtained in the single-site coherent-potential approximation

(CPA).^{10,11} (For an extensive review of the CPA, see Ref. 12.) This leads us to a 2×2 matrix equation for the elements of the effective-medium Green's function and self-energy matrices which must be solved self-consistently. The effective-medium Green's function is obtained formally in Sec. IV. In Sec. V we first obtain the phonon spectral density and electron MSD in the case of the perfect lattice in the presence of a magnetic field. This case provides a useful introduction to the more complicated case of the lattice in the presence of the pinning centers. In the latter case the phonon spectral density is obtained from the numerical solution of the self-consistent CPA equations derived in Sec. III.

II. THE HAMILTONIAN

In this paper we consider a 2D electron lattice in the presence of a static magnetic field, directed normally to the plane of the lattice, and an array of pinning centers placed at random at the sites of an otherwise perfect ideal lattice. Let us denote by $\bar{x}_{||}(l)$ the equilibrium position of the l th electron in the lattice. We have that

$$\bar{x}_{||}(l) = l_1 \bar{a}_1 + l_2 \bar{a}_2, \quad (2.1)$$

where \bar{a}_1 and \bar{a}_2 are the primitive translation vectors of the 2D electron lattice and l_1 and l_2 (referred to collectively as l) are any two integers (positive, negative, or zero). The instantaneous electron positions are given by the vectors

$$\bar{R}_{||}(l) = \bar{x}_{||}(l) + \bar{u}(l), \quad (2.2)$$

where we have denoted by $\bar{u}(l)$ the 2D displacement from equilibrium of the l th electron.

The Hamiltonian of our system is given by

$$H = H_{\text{har}} + H_1, \quad (2.3)$$

where

$$H_{\text{har}} = \frac{1}{2m^*} \sum_{l,\alpha} \Pi_{\alpha}^2(l) + \frac{1}{2} \sum_{l,\alpha} \sum_{l',\beta} \Phi_{\alpha\beta}(ll') u_{\alpha}(l) u_{\beta}(l') \quad (2.4)$$

is the Hamiltonian for the perfect lattice (in the harmonic approximation) in the presence of the magnetic field, and

$$H_1 = \frac{\gamma}{2} \sum_{l,\alpha} c(l) u_{\alpha}^2(l), \quad (2.5)$$

with

$$c(l) = \begin{cases} 1 & \text{if } l \text{ is a pinning site} \\ 0 & \text{otherwise} \end{cases} \quad (2.6)$$

is the Hamiltonian for the pinning centers.

In Eq. (2.4) we have denoted by $\Phi_{\alpha,\beta}(ll')$ the force-constant tensor for a 2D crystal of electrons interacting via the full Coulomb interaction.¹³ We have also denoted by $\Pi_{\alpha}(l)$ the α Cartesian component (in this paper greek indices denote Cartesian components x,y) of the momentum of an electron (whose effective mass and charge are m^* and $-e$, respectively),

$$\Pi_{\alpha}(l) = p_{\alpha}(l) + \frac{e}{c} A_{\alpha}(l), \quad (2.7)$$

where $p_{\alpha}(l)$ is the electron momentum in the absence of the magnetic field. The vector potential $\vec{A}(l) \equiv \vec{A}(\vec{R}_{||}(l))$ is taken in the Landau gauge, i.e.,

$$\vec{A}(l) = B(0, R_x(l), 0), \quad (2.8)$$

where B is the magnitude of the external magnetic field (directed along the z axis).

As indicated in the Introduction, the impurities that are present at the semiconductor-oxide interface at which we have assumed the existence of a 2D electron crystal are here modeled by a random array of "springs" of spring constant γ [see Eq. (2.5)]. One end of each of these springs is attached to a lattice site (pinning site) and the other end is attached to a point fixed in space (a heavy impurity). The latter feature of our model implies the existence of a "frame of reference," which has as a consequence the breaking of the infinitesimal translational invariance that characterizes the perfect lattice (described by H_{har}). The study of the implications of this breaking of translational symmetry for the localization of an electron about its lattice site is one of the main objectives of this work.

We note that the more realistic model (alluded to in the Introduction) in which the lattice is statically distorted by the presence of the pinning centers shares with our simpler model the physical feature of the breaking of infinitesimal translational invariance. Thus our results for the electron MSD given below should give an order-of-magnitude estimate for the results that would be obtained for a statically distorted lattice.

The model Hamiltonian introduced above is supplemented by the following commutation relations:

$$[u_{\alpha}(l), u_{\beta}(l')] = 0, \quad (2.9)$$

$$[\Pi_{\alpha}(l), u_{\beta}(l')] = -i\hbar\delta_{ll'}\delta_{\alpha\beta}, \quad (2.10)$$

and

$$[\Pi_{\alpha}(l), \Pi_{\beta}(l')] = -i\hbar m^* \omega_c \delta_{ll'} \epsilon_{\alpha\beta}, \quad (2.11)$$

where

$$\omega_c = \frac{eB}{m^*c}$$

is the cyclotron frequency of the electrons and the 2×2 matrix $\epsilon_{\alpha\beta}$ is defined by

$$\epsilon_{\alpha\beta} = \begin{cases} 1 & \text{if } \alpha=x, \beta=y \\ -1 & \text{if } \alpha=y, \beta=x \\ 0 & \text{if } \alpha=\beta. \end{cases} \quad (2.12)$$

III. PHONON GREEN'S FUNCTION AND ITS AVERAGE IN THE COHERENT-POTENTIAL APPROXIMATION

A. Self-consistent problem

We introduce the retarded (advanced) phonon Green's functions by the usual definitions

$$G_{\alpha\beta}^{(\pm)}(ll' | t) = \mp i \theta(\pm t) \langle [u_{\alpha}(lt), u_{\beta}(l'0)]_{\pm} \rangle, \quad (3.1)$$

where the upper (lower) sign defines the retarded (advanced) Green's function. In Eq. (3.1), $\theta(x)$ is the unit step function and the angular brackets denote the thermodynamic average over a canonical ensemble defined by the full Hamiltonian given in Eq. (2.3).

The equation of motion satisfied by the Fourier transform of $G_{\alpha\beta}^{(\pm)}(ll' | t)$ in the complex frequency plane, $G_{\alpha\beta}(ll' | z)$, can be readily shown to be

$$\sum_{l'',\gamma} [L_{\alpha\gamma}(ll'' | z) - \hbar V_{\alpha\gamma}(ll'')] G_{\gamma\beta}(l''l' | z) = \hbar \delta_{ll'} \delta_{\alpha\beta}, \quad (3.2)$$

where the operator $L_{\alpha\beta}(ll' | z)$ is given by the equation,

$$L_{\alpha\beta}(ll' | z) = m^* z^2 \delta_{ll'} \delta_{\alpha\beta} - \Phi_{\alpha\beta}(ll') + im^* \omega_c z \delta_{ll'} \epsilon_{\alpha\beta}, \quad (3.3)$$

and the (random) scattering potential $V_{\alpha\beta}(ll')$ is defined by

$$V_{\alpha\beta}(ll') = \frac{\gamma}{\hbar} c(l) \delta_{ll'} \delta_{\alpha\beta}. \quad (3.4)$$

In the remainder of this section we simplify the presentation by using matrix notation, defined such that $G_{\alpha\beta}(ll' | z) \equiv G(z)$, $V_{\alpha\beta}(ll') = V$, etc. [The matrix indices are, however displayed occasionally for clarity, for example, in Eqs. (3.15) and (3.16).]

It is a straightforward exercise to establish the Dyson equation relating $G(z)$ and $P(z)$, the Green's function appropriate to the perfect lattice [i.e., the solution to Eq. (3.2) in the absence of the pinning potential], namely,

$$G(z) = P(z) + P(z)VG(z). \quad (3.5)$$

While $P(z)$ describes the propagation of the phonons of the perfect lattice (in the presence of the magnetic field), $G(z)$ describes the propagation of the phonons in the "imperfect" lattice. Their scattering by the random pinning potential V introduces both self-energy corrections to their dispersion relations and finite lifetimes (or damping) of the phonon modes.

The average of Eq. (3.5) over all possible configurations of pinning centers can be formally taken by defining the self-energy $\Sigma(z) [\equiv \Sigma_{\alpha\beta}(ll' | z)]$ such that

$$\langle G(z) \rangle = P(z) + P(z)\Sigma(z)\langle G(z) \rangle. \quad (3.6)$$

In this work we obtain $\langle G(z) \rangle$ [or the self-energy $\Sigma(z)$] within the CPA.¹⁰⁻¹² We introduce the so-called effective-medium Green's function $G^{(0)}(z) [\equiv G_{\alpha\beta}^{(0)}(ll' | z)]$ and its associated self-energy $\hat{\Sigma}(z) [\equiv \hat{\Sigma}_{\alpha\beta}(ll' | z)]$ by the equation,

$$G^{(0)}(z) = P(z) + P(z)\hat{\Sigma}(z)G^{(0)}(z). \quad (3.7)$$

From Eqs. (3.6) and (3.7) we have that

$$G(z) = G^{(0)}(z) + G^{(0)}(z)[V - \hat{\Sigma}(z)]G(z). \quad (3.8)$$

We next introduce the scattering matrix $T(z) [= T_{\alpha\beta}(ll' | z)]$, defined such that Eq. (3.8) has the formal solution

$$G(z) = G^{(0)}(z) + G^{(0)}(z)T(z)G^{(0)}(z). \quad (3.9)$$

From Eqs. (3.8) and (3.9) we obtain the Dyson equation for the scattering matrix, namely,

$$T(z) = W(z) + W(z)G^{(0)}(z)T(z), \quad (3.10)$$

where we have made the definition

$$W(z) = V - \hat{\Sigma}(z). \quad (3.11)$$

At this point we can define the effective-medium Green's function more fully. We do so by requiring that

$$\mathcal{T}_{\alpha\beta}(z) = c \sum_{\alpha_1} W_{\alpha\alpha_1}^{(1)}(z) [\vec{I} - \vec{\mathcal{G}}^{(0)}(z) \vec{W}^{(1)}(z)]_{\alpha_1\beta}^{-1} + (1-c) \sum_{\alpha_1} W_{\alpha\alpha_1}^{(2)}(z) [\vec{I} - \vec{\mathcal{G}}^{(0)}(z) \vec{W}^{(2)}(z)]_{\alpha_1\beta}^{-1}. \quad (3.17)$$

In Eq. (3.17) we have introduced the following definitions:

$$\mathcal{G}_{\alpha\beta}^{(0)}(z) = G_{\alpha\beta}^{(0)}(ll | z), \quad (3.18)$$

where the notation emphasizes the fact that $G_{\alpha\beta}^{(0)}(ll | z)$ is independent of the lattice site l (by definition of the effective medium),

$$W_{\alpha\beta}^{(1)}(z) = \frac{\gamma}{\hbar} [\delta_{\alpha\beta} - \tilde{\Sigma}_{\alpha\beta}(z)] \quad (3.19)$$

and

$$W_{\alpha\beta}^{(2)}(z) = -\frac{\gamma}{\hbar} \tilde{\Sigma}_{\alpha\beta}(z). \quad (3.20)$$

$$\langle G(z) \rangle = G^{(0)}(z), \quad (3.12)$$

from which it follows that $\Sigma(z) = \hat{\Sigma}(z)$. According to Eq. (3.9), we must then have that

$$\langle T(z) \rangle = 0. \quad (3.13)$$

The physical content of the above procedure is clear. The actual disordered medium (described by the Green's function G) is replaced by an effective medium [described by the Green's function $G^{(0)}$] with an effective scattering center at every site except for those sites that are occupied by the real scattering (pinning) centers. The effective medium is determined by the condition that the scattering off the real scatterers vanishes on the average.

The prescription just outlined is implemented by solving Eq. (3.10) (or rather its average) by iteration. We have that

$$T(z) = W(z) + W(z)G^{(0)}(z)W(z) + \dots \quad (3.14)$$

We now make the simplifying (and rather usual) approximation of neglecting multiple scattering from two or more sites, while summing to all orders the scattering from one and the same site. This is the single-site CPA.

Inspection of Eq. (3.14) reveals that in this approximation the self-energy matrix $\hat{\Sigma}(z)$ must be diagonal in the indices l and l' . Thus we introduce the 2×2 self-energy matrix $\tilde{\Sigma}_{\alpha\beta}(z)$ by the equation

$$\hat{\Sigma}_{\alpha\beta}(ll' | z) = \frac{\gamma}{\hbar} \tilde{\Sigma}_{\alpha\beta}(z) \delta_{ll'}. \quad (3.15)$$

Taking the average of Eq. (3.14) term by term, after some algebra we are led to the result that

$$\langle T_{\alpha\beta}(ll' | z) \rangle = \mathcal{T}_{\alpha\beta}(z) \delta_{ll'}, \quad (3.16)$$

where

Thus, in the single-site approximation, the CPA condition given by Eq. (3.13) reduces to the 2×2 matrix equation given by

$$\mathcal{T}_{\alpha\beta}(z) = 0. \quad (3.21)$$

Now, according to the result given by Eq. (3.17), the elements of the scattering matrix $\mathcal{T}_{\alpha\beta}(z)$ are functions of the elements of the effective-medium Green's function $\mathcal{G}_{\alpha\beta}^{(0)}(z)$ and of the self-energy $\tilde{\Sigma}_{\alpha\beta}(z)$. Since the elements of $\mathcal{G}_{\alpha\beta}^{(0)}(z)$ are functionals of the elements of $\tilde{\Sigma}_{\alpha\beta}(z)$, Eqs. (3.17) and (3.21) define a self-consistent problem. This problem is solved in Sec. VI.

B. Electron MSD

The effective-medium Green's function defined above is the basic ingredient for the study of various thermodynamic and correlation functions for the imperfect 2D electron lattice. For example, from a knowledge of $\mathcal{G}_{\alpha\beta}^{(0)}(z)$ we can obtain the MSD of an electron about its equilibrium lattice site, averaged over all possible distributions of pinning centers. From standard results of thermodynamic Green's function theory we have that

$$\langle \langle u_{\alpha}^2(l) \rangle \rangle = \frac{1}{\pi} \int_0^{\infty} d\omega \coth \left[\frac{\beta \hbar \omega}{2} \right] \times \text{Im} \mathcal{G}_{\alpha\alpha}^{(0)}(z = \omega - i\eta), \quad (3.22)$$

where the notation emphasizes the fact that we have taken the average of the MSD (in the CPA) over all possible configurations of pinning centers. In Eq. (3.22) and elsewhere in this paper, the frequency ω is real.

In Sec. V we give explicit results for $\langle \langle u_{\alpha}^2(l) \rangle \rangle$ (which is, of course, independent of l). We note that the properties of the system enter Eq. (3.22) entirely via $\text{Im} \mathcal{G}_{\alpha\alpha}^{(0)}(z = \omega - i\eta)$, the phonon spectral density for the imperfect 2D electron crystal. This spectral density is obtained in Sec. V by solving the self-consistent CPA problem posed by Eq. (3.21).

We note that for $T=0$, Eq. (3.22) reduces to

$$\langle \langle u_{\alpha}^2(l) \rangle \rangle_{T=0} = \frac{1}{\pi} \int_0^{\infty} d\omega \text{Im} \mathcal{G}_{\alpha\alpha}^{(0)}(z = \omega - i\eta). \quad (3.23)$$

Thus for $T=0$ K the electron MSD is proportional to the area under the curve for the phonon spectral density (and this is always finite).

For any nonzero temperature we have that $\coth(\beta \hbar \omega / 2) \rightarrow 2k_B T / \hbar \omega$ as $\omega \rightarrow 0$. Thus if the phonon spectral density is finite (nonzero) at $\omega=0$, the integrand of Eq. (3.22) behaves like ω^{-1} for $\omega \rightarrow 0$ and the MSD diverges. As we shall see in Sec. V, that is the case for the perfect lattice (i.e., in the absence of the pinning centers).

We close this section by noting that the CPA provides the framework for the evaluation of the so-called conditional Green's functions.¹² In our case it is useful to introduce Green's functions $G_{\alpha\beta}^{(p)}(ll' | z)$ and $G_{\alpha\beta}^{(n)}(ll' | z)$ defined such that they equal the full Green's function $G_{\alpha\beta}(ll' | z)$ if l is, respectively, a pinning or a nonpinning site, and they vanish otherwise. The average of these new Green's functions over all possible configurations of pinning centers is

directly obtainable from the solution of the CPA problem [i.e., from the knowledge of $\mathcal{G}_{\alpha\beta}^{(0)}(z)$ and $\tilde{\Sigma}_{\alpha\beta}(z)$]. Equation (3.22) can then be used (replacing $\text{Im}G^{(0)}$ by $\text{Im}G^{(p)}$ and $\text{Im}G^{(n)}$, respectively) to compute the separate MSD for both the pinning and nonpinning sites (see Sec. V).

IV. EFFECTIVE-MEDIUM GREEN'S FUNCTION

In this section we obtain a formal result for the effective-medium Green's function defined in Sec. III. We begin by obtaining the Green's function for the perfect lattice in the presence of a dc magnetic field, $P_{\alpha\beta}(ll' | z)$ [the solution to Eq. (3.2) with $V=0$]. We make use of the translational invariance of the perfect lattice and introduce the 2D Fourier transform $P_{\alpha\beta}(\vec{q} | z)$ by the equation

$$P_{\alpha\beta}(ll' | z) = \frac{1}{N} \sum_{\vec{q}}^{\text{BZ}} \exp\{i\vec{q} \cdot [\vec{x}_{||}(l) - \vec{x}_{||}(l')]\} \times P_{\alpha\beta}(\vec{q} | z), \quad (4.1)$$

where N is the number of electrons in the lattice, and the sum runs over the first Brillouin zone (BZ) of the reciprocal lattice. In Eq. (4.1) and elsewhere in this paper, all wave vectors are 2D wave vectors in the plane of the lattice.

We next expand $P_{\alpha\beta}(\vec{q} | z)$ in the basis spanned by the eigenvectors $\vec{e}(\vec{q} | j)$ ($j=1,2$) of the dynamical matrix¹³ of the perfect 2D electron lattice in the absence of the magnetic field, that is, we set

$$P_{\alpha\beta}(\vec{q} | z) = \sum_{j=1}^2 \sum_{j'=1}^2 P_{jj'}(\vec{q} | z) e_{\alpha}(\vec{q} | j) e_{\beta}(\vec{q} | j'). \quad (4.2)$$

We recall that the eigenvalue of the dynamical matrix associated with the eigenvector $\vec{e}(\vec{q} | j)$ is the square of the frequency $\omega_j(\vec{q})$ of the j th phonon branch.¹³

Substituting Eqs. (4.1) and (4.2) in Eq. (3.2) (with $V=0$) and carrying out standard manipulations,¹⁴ we obtain the result that

$$P_{jj'}(\vec{q} | z) = \frac{\hbar}{m^*} \{ [z^2 - \omega_j^2(\vec{q})] \vec{I} + i\omega_c z \vec{E} \}_{jj'}^{-1}, \quad (4.3)$$

where the 2×2 matrix \vec{E} is defined by the equation

$$\vec{E}_{jj'} = \begin{cases} -1 & \text{if } j=1, j'=2 \\ 1 & \text{if } j=2, j'=1 \\ 0 & \text{if } j=j'. \end{cases} \quad (4.4)$$

Now in the single-site CPA problem of Sec. III we require the effective-medium Green's function (and

thus the perfect lattice Green's function) for $l'=l$ only. In that case we have

$$P_{\alpha\beta}(ll' | z) = \frac{1}{N} \sum_{\vec{q}} \sum_{j,j'=1}^2 P_{jj'}(\vec{q} | z) e_{\alpha}(\vec{q} | j) e_{\beta}(\vec{q} | j') \quad (4.5a)$$

$$\equiv \mathcal{P}_{\alpha\beta}(z) . \quad (4.5b)$$

At this point we restrict the discussion to the case of a hexagonal electron lattice. (This is the lattice structure observed in the experiments of Grimes and Adams² in the case of electrons at the surface of liquid helium.)

On the basis of the transformation properties of the perfect lattice Green's function under the operations of the point group of the hexagonal lattice (the group C_{6v}), we can show the results that¹⁵

$$\mathcal{P}_{xx}(z) = \mathcal{P}_{yy}(z) \quad (4.6a)$$

and

$$\mathcal{P}_{xy}(z) = -\mathcal{P}_{yx}(z) . \quad (4.6b)$$

Substituting Eqs. (4.3) and (4.6) in Eq. (4.5) and making use of the orthogonality of the eigenvectors $e_{\alpha}(\vec{q} | j)$ (in addition to the result quoted in Ref. 14), we obtain the following results for the two independent elements of the perfect lattice Green's function for $l'=l$:

$$\mathcal{P}_{xx}(z) = \frac{\hbar}{2m^*N} \sum_{\vec{q}} \frac{2z^2 - \Omega_1^2(\vec{q}) - \Omega_2^2(\vec{q}) + \omega_c^2}{[z^2 - \Omega_1^2(\vec{q})][z^2 - \Omega_2^2(\vec{q})]} \quad (4.7a)$$

and

$$\mathcal{P}_{xy}(z) = -\frac{\hbar}{m^*N} \sum_{\vec{q}} \frac{i\omega_c z}{[z^2 - \Omega_1^2(\vec{q})][z^2 - \Omega_2^2(\vec{q})]} , \quad (4.7b)$$

$$\mathcal{G}_{xx}^{(0)}(z) = \frac{\hbar}{2m^*N} \sum_{\vec{q}} \frac{2z^2 - \Omega_1^2(\vec{q}) - \Omega_2^2(\vec{q}) + \omega_c^2 - 2(\gamma/m^*)\tilde{\Sigma}_{xx}(z)}{\Delta(\vec{q} | z)} \quad (4.10a)$$

and

$$\mathcal{G}_{xy}^{(0)}(z) = -\frac{\hbar}{m^*N} \sum_{\vec{q}} \frac{i\omega_c z - (\gamma/m^*)\tilde{\Sigma}_{xy}(z)}{\Delta(\vec{q} | z)} , \quad (4.10b)$$

where the function $\Delta(\vec{q} | z)$ is defined by

$$\Delta(\vec{q} | z) = \left[i\omega_c z - \frac{\gamma}{m^*} \tilde{\Sigma}_{xy}(z) \right]^2 + \left[z^2 - \omega_1^2(\vec{q}) - \frac{\gamma}{m^*} \tilde{\Sigma}_{xx}(z) \right] \left[z^2 - \omega_2^2(\vec{q}) - \frac{\gamma}{m^*} \tilde{\Sigma}_{xx}(z) \right] . \quad (4.11)$$

where $\Omega_j(\vec{q})$, $j=1,2$, are the phonon frequencies in the presence of the magnetic field [the poles of $\mathcal{P}_{\alpha\beta}(z)$]. They are related to $\omega_j(\vec{q})$ (the phonon frequencies in the absence of the field) by the equation

$$\begin{aligned} \Omega_{1,2}^2(\vec{q}) &= \frac{1}{2} [\omega_c^2 + \omega_1^2(\vec{q}) + \omega_2^2(\vec{q})] \\ &\pm \left\{ \frac{1}{4} [\omega_c^2 + \omega_1^2(\vec{q}) + \omega_2^2(\vec{q})]^2 \right. \\ &\quad \left. - \omega_1^2(\vec{q})\omega_2^2(\vec{q}) \right\}^{1/2} . \end{aligned} \quad (4.8)$$

The effective-medium Green's function $G_{\alpha\beta}^{(0)}(ll' | z)$ is obtained by solving the Dyson equation (3.7), and this is done by transforming Eq. (3.7) into a matrix equation for the coefficients $G_{jj'}^{(0)}(\vec{q} | z)$, defined according to Eqs. (4.1) and (4.2). The solution to that matrix equation gives $G_{jj'}^{(0)}(\vec{q} | z)$ in terms of $P_{jj'}(q | z)$ [given by Eq. (4.3)]. For brevity here we do not display that result. [The same is implicit in the main result of this section, Eq. (4.10).]

At this point it is convenient again to restrict our discussion to the case of the hexagonal lattice. We require that the transformation properties of the effective-medium Green's function under the symmetry operations of the point group of the hexagonal lattice be the same as those of the perfect lattice Green's function. In this case we have that [cf. Eqs. (3.18) and (4.6a)]

$$\mathcal{G}_{xx}^{(0)}(z) = \mathcal{G}_{yy}^{(0)}(z) \quad (4.9a)$$

and

$$\mathcal{G}_{xy}^{(0)}(z) = -\mathcal{G}_{yx}^{(0)}(z) , \quad (4.9b)$$

with similar equations relating the elements of the self-energy matrix $\tilde{\Sigma}_{\alpha\beta}(z)$.

The above comments provide the outline for the derivation of the following results for the two independent elements of the effective-medium Green's function $\mathcal{G}_{\alpha\beta}^{(0)}(z)$:

Note that the only dependence on the wave vector \vec{q} of the argument of the above sums is through the phonon frequencies $\Omega_j(\vec{q})$. [In other words, the eigenvectors $\vec{e}(\vec{q} | j)$ have been eliminated from our results for the elements of $\mathcal{G}_{\alpha\beta}^{(0)}(z)$.] This is very useful since then, in the computation of $\mathcal{G}_{\alpha\beta}^{(0)}(z)$, we only need to diagonalize the dynamical matrix in the irreducible element of the BZ for the hexagonal lattice. The result given by Eq. (4.10) together with the CPA equation (3.21) constitutes the self-consistent problem solved in Sec. V.

V. RESULTS AND DISCUSSIONS

In this section we present detailed numerical results for the phonon spectral density and the electron MSD obtained on the basis of the theory formulated in the previous sections. It is useful to consider separately the following three cases: (a) the perfect lattice in a magnetic field; (b) the lattice with pinning centers without a magnetic field; (c) the lat-

tice in the presence of both the magnetic field and the pinning centers.

A. Perfect lattice in the presence of a dc magnetic field normal to the plane of the lattice

The present physical system has been studied before. However, the published work refers only to some results for the phonon dispersion relations^{5-8,16} or to qualitative results for the electron MSD.⁸ Our results for the phonon spectral density given below illustrate the physics of the system rather clearly and serve as a useful reference for the results obtained later in the presence of disorder.

In the present case the phonon Green's function is the perfect-medium Green's function $P_{\alpha\beta}(l' | z)$ obtained in Sec. IV. For $l'=l$ we have the explicit results given by Eqs. (4.6) and (4.7). Here we shall mainly discuss the phonon spectral density. From Eq. (4.7) it follows that

$$\text{Im}\mathcal{P}_{xx}(z=\omega-i\eta) = \frac{\pi\hbar}{2m^*N} \sum_{\vec{q}} \frac{2\omega^2 - \Omega_1^2(\vec{q}) - \Omega_2^2(\vec{q}) + \omega_c^2}{\Omega_1^2(\vec{q}) - \Omega_2^2(\vec{q})} \left[\frac{\delta(\omega - \Omega_1(\vec{q}))}{\omega + \Omega_1(\vec{q})} - \frac{\delta(\omega - \Omega_2(\vec{q}))}{\omega + \Omega_2(\vec{q})} \right]. \quad (5.1)$$

We can readily verify the result that¹⁷

$$\int_0^\infty d\omega \omega \text{Im}\mathcal{P}_{xx}(z=\omega-i\eta) = \frac{\pi}{2} \frac{\hbar}{m^*}. \quad (5.2)$$

We have computed the frequencies $\Omega_j(\vec{q})$ by first diagonalizing the dynamical matrix appropriate to a hexagonal electron lattice, for which a rapidly convergent result has been given by Bonsall and Maradudin.¹³ The eigenvalues of the dynamical matrix give us the frequencies $\omega_j(\vec{q})$ of the phonons in the absence of the magnetic field. The corresponding frequencies in the presence of the field $\Omega_j(\vec{q})$ are then obtained from Eq. (4.8).

Now since the frequencies $\omega_j(\vec{q})$ have the full symmetry of the point group of the hexagonal lattice, we only need to carry out the above computa-

tion within the irreducible element of the BZ of the reciprocal lattice (shown in Fig. 1). The sum over the whole BZ required in Eq. (5.1) is then carried out by assigning each point inside its irreducible element an appropriate weight (determined by symmetry). Typically, we have computed the frequencies $\omega_j(\vec{q})$ at the points of a fine mesh of 456 points in the irreducible element of the BZ (the corresponding

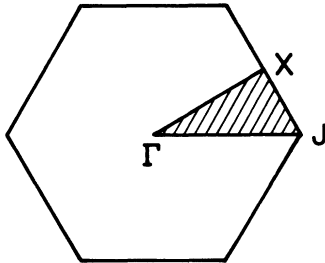


FIG. 1. First BZ for the 2D hexagonal lattice. The shaded area is the irreducible element of this zone.

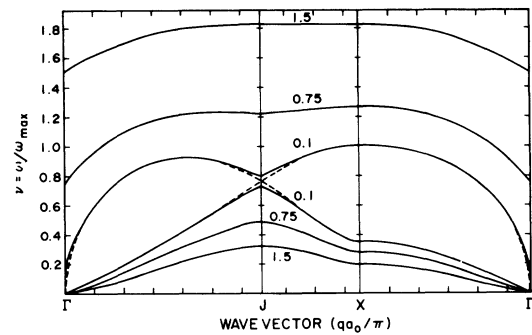


FIG. 2. Phonon dispersion curves for a 2D hexagonal electron lattice in a dc magnetic field perpendicular to the plane of the lattice for wave vectors along the boundary of the irreducible element of the first BZ. The curves shown correspond to three values of the reduced cyclotron frequency $\nu_c = \omega_c/\omega_{\max}$ (ω_{\max} being the maximum frequency of the crystal in the absence of the magnetic field). The dashes indicate the dispersion curves for $\nu_c=0$, which differ from the dispersion curves for $\nu_c=0.1$ only near the Γ and J points, as shown.

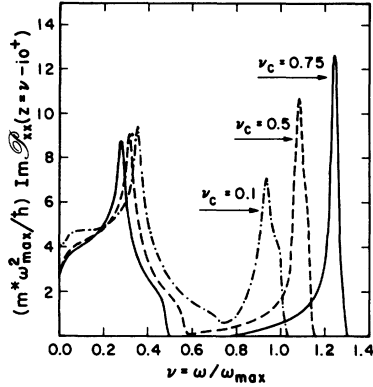


FIG. 3. Phonon spectral density for a perfect 2D hexagonal electron lattice in the presence of a dc magnetic field perpendicular to the plane of the lattice, for three values of the reduced cyclotron frequency $\nu_c = \omega_c / \omega_{max}$.

number of points in the entire BZ is 5041).

In Fig. 2 we show the phonon dispersion curves for wave vectors along the boundary of the irreducible element of the BZ for three values of the reduced cyclotron frequency ν_c defined by the equation

$$\nu_c = \frac{\omega_c}{\omega_{max}}, \quad (5.3)$$

where ω_{max} is the maximum frequency of the crystal in the absence of the magnetic field (which occurs at the X point in the first BZ), and is given by

$$\omega_{max} \cong 1.256\omega_p. \quad (5.4)$$

Here ω_p is the “plasma” frequency of the 2D electron crystal, defined according to the equation

$$\omega_p^2 = \frac{2\pi e^2 n_s}{m^* \bar{\epsilon} a_0}, \quad (5.5)$$

where a_0 is the interelectron distance, n_s is the areal electron density [$n_s = 2/(\sqrt{3}a_0^2)$], and $\bar{\epsilon}$ is the effective

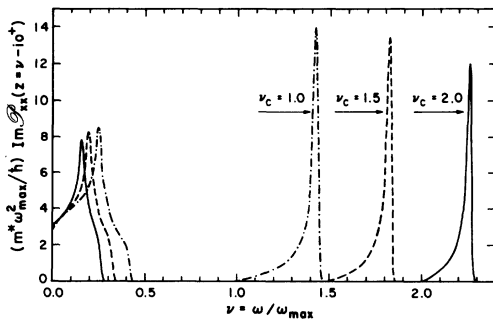


FIG. 4. Same as Fig. 3, but for larger values of the reduced cyclotron frequency ν_c . Note that the (nonzero) value of the phonon spectral density at zero frequency is rather insensitive to the value of ν_c [see comment below Eq. (3.23)].

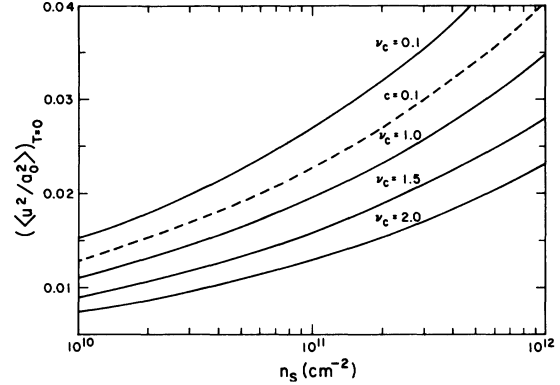


FIG. 5. MSD of an electron in a perfect 2D hexagonal lattice at $T=0$ K in the presence of a dc magnetic field perpendicular to the plane of the lattice, in units of a_0^2 (a_0 being the interelectron distance), as a function of the areal electron density. The curves are labeled by the corresponding value of the reduced cyclotron frequency ν_c . The curve for $\nu_c=0.1$ almost coincides with the curve that obtains for $\nu_c=0$ (i.e., in the absence of the magnetic field). The dashed curve corresponds to the field-free lattice in the presence of a random array of pinning centers of concentration $c=0.1$ and pinning strength $\lambda=1$ [see Eq. (5.10)].

dielectric constant of the interface for the electrons in the 2D crystal. [$\bar{\epsilon} = (\epsilon_1 + \epsilon_2)/2$, where ϵ_1 and ϵ_2 are the dielectric constants of the semiconductor and the oxide layer, respectively, in the case of a Wigner crystal at a semiconductor-oxide interface.]

Note that ν_c is a function of both the external magnetic field and the electron density. In the case of the silicon–silicon-oxide interface we have that

$$\nu_c \cong 0.718 \frac{b}{N_s^{3/4}}, \quad (5.6)$$

where b is the magnitude of the magnetic field in teslas ($1 \text{ T} = 10^4 \text{ G}$) and N_s is the electron density in units of 10^{10} cm^{-2} . Thus in the small density region ($N_s \cong 1$), with moderate values of b we can achieve fairly large values of ν_c .

The main features of the dispersion curves shown in Fig. 2 are easily visualized. While in the absence of the magnetic field the frequency $\omega_l(\vec{q})$ of the longitudinal phonon mode behaves like $q^{1/2}$ as $q \rightarrow 0$, in the presence of the field we have that $\Omega_l(\vec{q}) = \omega_c$ for $q=0$. For the transverse phonon we have that¹⁸ $\Omega_t(\vec{q}) \sim q^{3/2}$ for $q \rightarrow 0$. We also find that the magnetic field removes the degeneracy that exists at the J point in the field-free case, as shown in Fig. 2. The magnitude of the gap created at the zone boundary increases with increasing values of ν_c , until an absolute gap develops between both phonon branches.

In Figs. 3 and 4 we give results for the phonon

spectral density for several values of ν_c .¹⁹ For $\nu_c=0.1$ the phonon spectral density is almost identical to that for $\nu_c=0$, i.e., to the field-free limit. The lower-frequency peak corresponds to the transverse phonon branch and the higher-frequency peak corresponds to the longitudinal phonon branch. For $\nu_c>0.5$ a gap develops between both peaks. Its magnitude increases with increasing values of ν_c . The existence of this gap is explained by the corresponding feature of the phonon dispersion curves discussed above.

From the point of view of this paper the main qualitative feature of Figs. 3 and 4 is that the phonon spectral density is finite at $\omega=0$. According to the comment that follows Eq. (3.23), this result immediately implies that the MSD of an electron diverges at any nonzero temperature.

In Fig. 5 we give results for the MSD at $T=0$ [computed using Eqs. (3.23) and (5.1)] for various values of ν_c as a function of the electron density. (Note that for the hexagonal lattice $\langle\langle u^2 \rangle\rangle=2\langle\langle u_x^2 \rangle\rangle$.) The stabilizing effect of the magnetic field at $T=0$ K (particularly at small areal densities) is apparent.

B. Lattice in the presence of a random array of pinning centers ($\vec{B}=0$)

The theory presented in Secs. II–IV simplifies considerably in the limit $\vec{B}=0$. From Eq. (4.7b) we have that $\mathcal{P}_{xy}(z)=0$ for $\omega_c=0$. Since we require that $\mathcal{G}_{\alpha\beta}^{(0)}(z)$ have the same symmetry properties²⁰ as $\mathcal{P}_{\alpha\beta}(z)$, it must then be the case that $\mathcal{G}_{xy}^{(0)}(z)=0$. According to Eq. (4.10b) we must also have that $\tilde{\Sigma}_{xy}(z)=0$. Thus when no magnetic field is present we have that

$$\mathcal{G}_{\alpha\beta}^{(0)}(z) = \mathcal{G}^{(0)}(z)\delta_{\alpha\beta} \quad (5.7)$$

and

$$\tilde{\Sigma}_{\alpha\beta}(z) = \tilde{\Sigma}(z)\delta_{\alpha\beta}. \quad (5.8)$$

The definition of the (scalar) effective-medium Green's function $\mathcal{G}^{(0)}(z)$ [as a functional of the scalar self-energy $\tilde{\Sigma}(z)$] is given by Eqs. (4.10a) and (4.11) upon setting $\omega_c=0$, $\tilde{\Sigma}_{xy}=0$.

Thus in the present case the CPA equation (3.21) reduces to a simpler scalar equation, which after a little algebra can be written as

$$\frac{\hbar}{\gamma}[c - \tilde{\Sigma}(z)] = \mathcal{G}^{(0)}(z)\tilde{\Sigma}(z)[\tilde{\Sigma}(z) - 1]. \quad (5.9)$$

The self-consistent problem was solved as follows.²¹ There are two dimensionless parameters in the problem, namely, the concentration c and the ratio

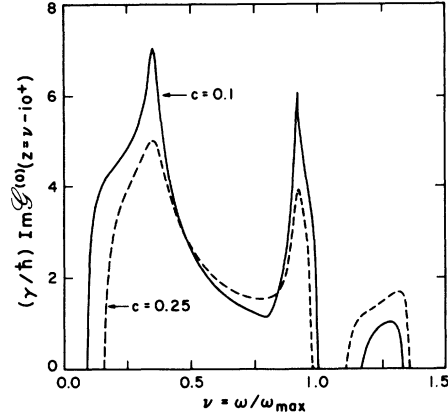


FIG. 6. Phonon spectral density $\text{Im} \mathcal{G}^{(0)}(z = \omega - i\eta)$ for a 2D hexagonal electron lattice in the presence of a random array of pinning centers for two values of the concentration c . Here the relative pinning strength λ [see Eq. (5.10)] equals unity. Note that the magnitude of the low-frequency gap and the width of the impurity band increase with the concentration.

$$\lambda^2 = \frac{m^* \omega_{\max}^2}{\gamma} \quad (5.10)$$

that characterizes the strength of the pinning potential. For small pinning strengths (λ large) we expect the virtual-crystal result $\text{Re} \tilde{\Sigma} = c$, $\text{Im} \tilde{\Sigma} = 0$ to be a good approximation. These limiting values of the self-energy were used (we actually used a small nonzero value for $\text{Im} \tilde{\Sigma}$) to start the iteration procedure that results from first computing $\mathcal{G}^{(0)}(z)$ and then solving Eq. (5.9) (Newton's method was used) to obtain a new value of the self-energy, and so on until convergence was achieved. This procedure was carried out for successively smaller values of λ .

In Fig. 6 we show the phonon spectral density $\text{Im} \mathcal{G}^{(0)}(z = \omega - i\eta)$ obtained by the above procedure for $c=0.1$ and $\lambda=1$. (For illustrative purposes in Fig. 6 we also show the results obtained for $c=0.25$.) We note that the choice $\lambda=1$ corresponds to a pinning strength such that the pinning parameter γ equals the effective spring constant for the maximum frequency in the crystal. This value of λ is relevant experimentally.⁴

The main new feature of the phonon spectral density shown in Fig. 6 is the presence of a low-frequency gap (cf. Figs. 3 and 4). This gap is a direct consequence of the breaking of the infinitesimal translational invariance that exists in the perfect lattice by the presence of the pinning centers. Thus the electron MSD is now finite at finite temperatures.

A second feature²² of Fig. 6 is the presence of an impurity band for frequencies greater than ω_{\max} . This result can be understood by considering the

problem of *one* pinning center in a perfect lattice. One can show that in that case, in addition to the continuous spectrum, there exists one isolated state bound to the pinning site. For $\lambda=1$ this bound state occurs at $\nu=\omega/\omega_{\max}\simeq 1.26$. When a finite concentration of pinning centers is present, this state turns into an impurity band, as shown in Fig. 6.

A check of the accuracy of our numerical solution is given by the sum rule (5.2). That $\mathcal{G}^{(0)}(z)$ satisfies this sum rule can be proved as follows. From Eq. (5.7) and the first paragraph below Eq. (5.8) we have that $\mathcal{G}^{(0)}(z)$ is analytic in the upper half-plane²³ and that for $|z| \rightarrow \infty$,

$$\mathcal{G}^{(0)}(z) \rightarrow \frac{\hbar}{m^*} \frac{1}{z^2}. \quad (5.11)$$

Then noting that the spectral density is an odd function of the frequency ω , and using Cauchy's theorem, we have that

$$\begin{aligned} \int_0^\infty d\omega \omega \operatorname{Im} \mathcal{G}^{(0)}(z=\omega-i\eta) \\ = -\frac{1}{2} \operatorname{Im} \int_{R_\infty} dz z \mathcal{G}^{(0)}(z), \end{aligned} \quad (5.12)$$

where the integral on the right-hand side is taken over a large semicircle on the upper half-plane. Substituting Eq. (5.11) into (5.12) we readily prove that the right-hand side of Eq. (5.12) equals $\pi\hbar/2m^*$. The spectral density shown in Fig. 6 satisfies the sum rule to better than 1% and we take this as a measure of the overall accuracy of our numerical procedure.

In Fig. 5 we give the MSD (note that $\langle\langle u^2 \rangle\rangle = 2\langle\langle u_x^2 \rangle\rangle$ for the hexagonal lattice) obtained by evaluating the integral in Eq. (3.23) with the use of the spectral density shown in Fig. 6 for $c=0.1$. (As indicated above, in the present case we can also compute the MSD at finite temperatures. For brevity we give the MSD at $T \neq 0$ in Sec. VC only.) Now the concentration of pinning centers in practice is restricted to small values. On the other hand, the reduced cyclotron frequency ν_c can be varied rather easily. Thus the results of Fig. 5 show that at $T=0$ the magnetic field by itself is a much more efficient mechanism for the localization of an electron about its lattice site than are the pinning centers by themselves.

Finally, we have evaluated the separate electron MSD for both pinning and nonpinning sites (in the manner outlined at the end of Sec. III). The conclusion is that the former is about 2 orders of magnitude smaller than the latter. We then expect that an external magnetic field will, through its effect on the nonpinning sites, bring about a further reduction in $\langle\langle u^2 \rangle\rangle$. This question is considered next.

C. Lattice in the presence of both a random array of pinning centers and an external magnetic field

The self-consistent problem to be solved is now given by Eqs. (3.17), (3.21), (4.10a), and (4.10b). In the case of the hexagonal lattice, using the symmetry relations given by Eqs. (4.9) [recall that similar equations relate the elements of $\tilde{\Sigma}_{\alpha\beta}(z)$] in Eq. (3.17) we can show that

$$\mathcal{T}_{xx}(z) = \mathcal{T}_{yy}(z) \quad (5.13a)$$

and

$$\mathcal{T}_{xy}(z) = -\mathcal{T}_{yx}(z). \quad (5.13b)$$

Thus in the present case we must solve a system of two CPA equations given by

$$\mathcal{T}_{xx}(z) = 0 \quad (5.14a)$$

and

$$\mathcal{T}_{xy}(z) = 0. \quad (5.14b)$$

Equations (5.14) were solved by Newton's method.²¹ The problem is self-consistent since $\mathcal{G}_{\alpha\beta}^{(0)}(z)$ and $\tilde{\Sigma}_{\alpha\beta}(z)$ are related by Eqs. (4.10). We began with a small value of the reduced cyclotron frequency ν_c , in which case the field-free results for the self-energy were used as input to the iteration procedure. We then increased ν_c by steps and at each step we used as input the results for the self-energy elements obtained for the previous value of ν_c . However, in the frequency regions near the gaps of the spectrum it became necessary to solve the CPA equations by

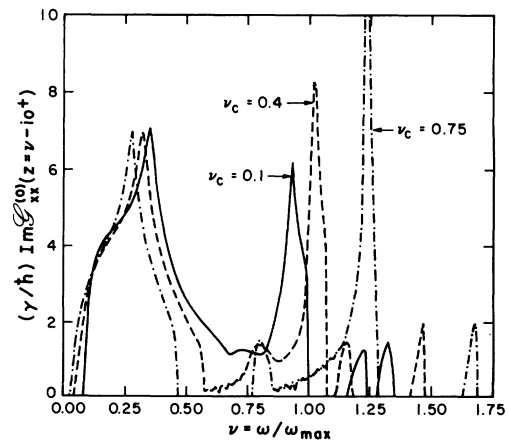


FIG. 7. Phonon spectral density $\operatorname{Im} \mathcal{G}_{xx}^{(0)}(z=\nu-i\eta)$ for a 2D hexagonal electron lattice in the presence of a magnetic field perpendicular to the plane of the lattice and a random array of pinning centers with concentration $c=0.1$ and relative pinning strength $\lambda=1$. The curves shown correspond to three values of the relative cyclotron frequency ν_c .

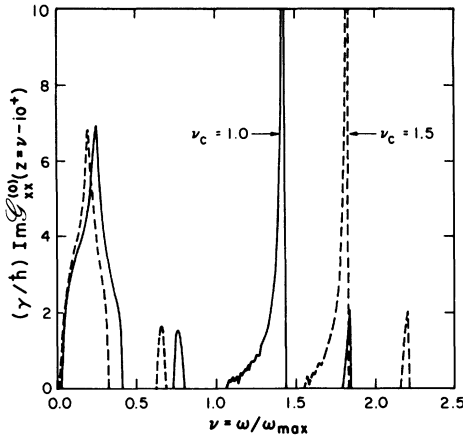


FIG. 8. Same as Fig. 7 but for higher values of ν_c . Note that for $\nu_c = 1.5$ the low-frequency gap disappears. Note also that since we have set $\lambda = 1$ [cf. Eq. (5.10)], the scales of Figs. 3, 4, and 6–8 are the same.

converging toward the gaps by varying the frequency ω by very small amounts (for a fixed ν_c).

It was verified that our numerical results for the phonon spectral density satisfy the sum rule (5.2) to 1% accuracy. [The proof that the result for $\mathcal{S}_{xx}^{(0)}(z)$ given by Eq. (4.10a) is consistent with Eq. (5.2) proceeds along similar lines to the one given earlier in the case that $\vec{B} = 0$.]

In Figs. 7 and 8 we show our results for the phonon spectral density $\text{Im} \mathcal{S}_{xx}^{(0)}(z = \omega - i\eta)$ for several values of ν_c . For $\nu_c = 0.1$, the spectral density resembles closely the corresponding result for $\nu_c = 0$ (given in Fig. 6), except that the impurity band that was present in the latter case has now split into two bands by the presence of the magnetic field.²⁴ For

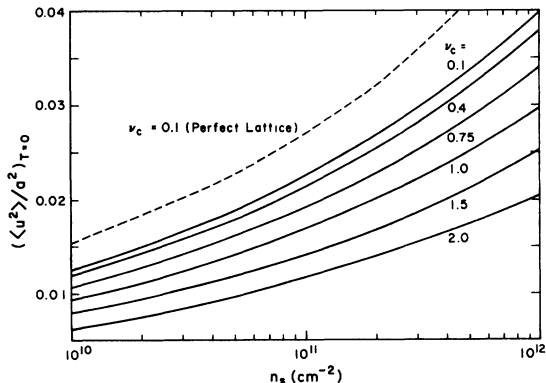


FIG. 9. MSD of an electron in a 2D electron lattice at $T = 0$ K in the presence of a dc magnetic field normal to the plane of the lattice and a random array of pinning centers, as a function of the areal electron density, for various values of the reduced cyclotron frequency ν_c . Here $c = 0.1$ and $\lambda = 1$. The dashed curve corresponds to the perfect lattice (no pinning centers) for $\nu_c = 0.1$.

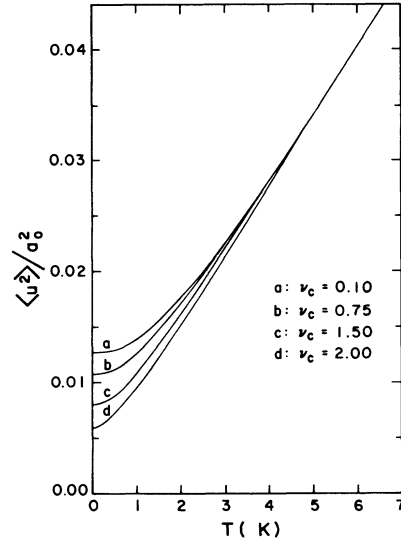


FIG. 10. MSD of an electron in a 2D electron lattice in the presence of a dc magnetic field normal to the plane of the lattice and a random array of pinning centers, as a function of temperature, for four values of the reduced cyclotron frequency ν_c . Here $n_s = 10^{10} \text{ cm}^{-2}$, $c = 0.1$, and $\lambda = 1$.

larger values of ν_c , the splitting between the impurity bands increases, and for $\nu_c \gtrsim 0.75$, the lower-lying impurity band occurs in the gap between the two phonon bands.

A striking feature of our results is that as ν_c is increased, the magnitude of the low-frequency gap increases, until for $\nu_c > 1.5$ this gap disappears (see Fig. 8). We interpret this result as follows. The low-frequency gap, is as noted before, a direct consequence of the breaking of translational invariance by the presence of the pinning centers. As ν_c is increased, the vibrational motion of the electrons is more and more quenched (the cyclotron radius decreases) and thus the electrons probe the presence of the pinning centers less effectively. However, we note that there remains residual information as to the presence of the pinning centers in that, although the low-frequency gap disappears, the phonon spectral density vanishes at zero frequency. (This result holds true for values of $\nu_c > 1.5$.) In fact, the spectral density vanishes sufficiently fast as $\omega \rightarrow 0$ that the MSD remains finite at finite temperatures.

In Fig. 9 we present results for the electron MSD at $T = 0$ K for various values of ν_c as a function of the electron areal density. For comparison we also give the plot for the MSD that obtains at $T = 0$ K in the case of the perfect lattice. From Fig. 9 we have that, first, the introduction of the pinning centers decreases the MSD as shown. Next, by increasing the magnetic field (keeping the concentration c fixed), the MSD is further decreased. We note that

for $n_s = 10^{10} \text{ cm}^{-2}$ and $v_c = 2.0$, Eq. (5.6) gives $b = 2.79$ (or $B = 2.79 \text{ T}$). Since values of B up to about 8 T are used in the experimental work in the field,⁴ we conclude that, at $T = 0 \text{ K}$, the combined effects of the pinning centers and the magnetic field considerably enhance the localization of the electrons about their equilibrium lattice sites.

It is instructive to view the results of Fig. 9 in the light of the Lindemann criterion of melting,²⁵ according to which the crystal would melt for $(\langle u^2 \rangle / a_0^2)_{T=0 \text{ K}} \cong (0.16)^2 = 0.0256$. At small densities ($n_s \sim 10^{10} \text{ cm}^{-2}$) this criterion is satisfied extremely well with moderate values of the magnetic field.

In Fig. 10 we present results for the electron MSD as a function of temperature for a given electron areal density ($n_s = 10^{10} \text{ cm}^{-2}$; we also set $c = 0.1$ and $\lambda = 1.0$). The main feature of Fig. 10 is worth a comment. In effect, while at $T = 0 \text{ K}$ we can decrease the MSD substantially by increasing the magnetic field (for a fixed concentration of pinning centers), the same does not hold true for temperatures above a few degrees kelvin. This result is explained as follows. From Eq. (3.23) we have that, in the high-temperature limit,

$$\begin{aligned} \langle \langle u^2 \rangle \rangle &= 2 \langle \langle u_x^2 \rangle \rangle \\ &\sim \frac{4k_B T}{\pi \hbar} \int_0^\infty d\omega \frac{\text{Im} \mathcal{G}_{xx}^{(0)}(z = \omega - i\eta)}{\omega}. \end{aligned} \quad (5.15)$$

From the well-known Kramers-Kronig relations satisfied by the Green's function defined in Sec. III (and thus by the effective-medium Green's function), we have that the coefficient of $k_B T$ in Eq. (5.15) is proportional to $\text{Re} \mathcal{G}_{xx}^{(0)}(\omega = 0)$. Our numerical solution for $\text{Re} \mathcal{G}_{xx}^{(0)}(\omega = 0)$ is independent of the value of the magnetic field. Thus according to Eq. (5.15) so is the MSD.

We note that the limit given by Eq. (5.15) becomes valid at (slightly) higher temperatures as we increase the magnetic field. This was to be expected from the dependence on the magnetic field of the

spectral densities shown in Figs. 7 and 8.

Finally, we have evaluated the separate electron MSD for both the pinning and nonpinning sites (cf. last paragraph of Sec. III). With the values of magnetic field for which we have obtained the phonon spectral densities, the MSD for the pinning sites is still much smaller than the MSD corresponding to the nonpinning sites.

VI. SUMMARY

We have obtained the phonon spectral density for a 2D electron lattice in the presence of a dc magnetic field and a random array of pinning centers. From a knowledge of the phonon spectral density we have computed the electron MSD. Although at sufficiently high values of the magnetic field the low-frequency gap in the phonon spectral density disappears (such a gap results from the presence of the pinning centers), the MSD remains finite at finite temperatures. At low temperatures ($T \lesssim 1 \text{ K}$), the MSD is reduced considerably below the value for which the Lindemann criterion would predict the melting of the lattice with rather moderate values of the magnetic field. At higher temperatures the value of the MSD is essentially determined by the value of the concentration of the pinning centers. From our results we conclude that for $T \lesssim 1 \text{ K}$ both the magnetic field and the pinning centers (without which $\langle u^2 \rangle = \infty$ for $T \neq 0$) considerably aid the stability of the 2D electron crystal.²⁶

ACKNOWLEDGMENTS

The work of one of the authors (A.A.M.) was begun while he was a visitor in the Department of Theoretical Physics at the University of Oxford, supported by the Science Research Council (United Kingdom). This support is gratefully acknowledged. We are grateful for useful discussions with Professor R. A. Tahir-Kheli and Dr. M. Prasad during the early stages of this work. This work was supported in part by National Science Foundation Grant No. DM-78-09430.

¹E. Wigner, Phys. Rev. **46**, 1002 (1934).

²C. C. Grimes and G. Adams, Phys. Rev. Lett. **42**, 795 (1979).

³For an exhaustive review of the properties of 2D electron systems, see T. Ando, A. B. Fowler, and F. Stern, Rev. Mod. Phys. **54**, 437 (1982).

⁴B. A. Wilson, S. J. Allen, Jr., and D. C. Tsui, Phys. Rev. B **24**, 5887 (1981).

⁵Yu. E. Lozovik and V. I. Yudson, Zh. Eksp. Teor. Fiz. Pis'ma Red. **22**, 26 (1975) [JETP Lett. **22**, 11 (1975)].

⁶H. Fukuyama, Solid State Commun. **17**, 1323 (1975); **19**, 551 (1976).

⁷Yu. E. Lozovik, D. R. Musin, and V. I. Yudson, Fiz. Tverd. Tela (Leningrad) **21**, 1974 (1979) [Sov. Phys.—Solid State **21**, 1132 (1979)].

⁸F. P. Ulinich and N. A. Usov, Zh. Eksp. Teor. Fiz. **76**, 288 (1979) [Sov. Phys.—JETP **49**, 147 (1979)].

⁹H. Fukuyama and P. A. Lee, Phys. Rev. B **18**, 6245 (1978).

¹⁰P. Soven, Phys. Rev. **156**, 1017 (1967).

¹¹D. W. Taylor, Phys. Rev. **156**, 1017 (1967).

¹²R. J. Elliott, J. A. Krumhansl, and P. L. Leath, Rev. Mod. Phys. **46**, 465 (1974).

¹³L. Bonsall and A. A. Maradudin, Phys. Rev. B **15**, 1959 (1977).

¹⁴We note that a nonobvious result needed in the derivation of Eq. (4.3) is given by the equation,

$$e_x(\vec{q} | j=1)e_y(\vec{q} | j=2) - e_x(\vec{q} | j=2)e_y(\vec{q} | j=1) = -1.$$

¹⁵A. A. Maradudin (unpublished).

¹⁶G. Meisner, Z. Phys. B **23**, 173 (1976).

¹⁷Equation (5.2) is a particular case of the first frequency-moment (or f -) sum rule satisfied by the spectral weight function associated with any two operators [in the present case the operators $u_x(lt)$ and $u_x(l0)$].

¹⁸See, e.g., Ref. 13. The limits of $\Omega_1(\vec{q})$ and $\Omega_2(\vec{q})$ for $\vec{q} \rightarrow 0$ are readily obtained from Eq. (4.8) and the corresponding results for $\omega_1(\vec{q})$ and $\omega_2(\vec{q})$ are obtained in Ref. 13.

¹⁹We note that in evaluating numerically the expression for $I_m \mathcal{P}_{xx}(z = \omega - i\eta)$ given by Eq. (5.1), we adopted the following representation for the delta function:

$$\delta(x) = \frac{1}{\sqrt{\pi}} \lim_{\epsilon \rightarrow 0} \frac{1}{\sqrt{\epsilon}} e^{-x^2/\epsilon}.$$

The results shown in Figs. 3 and 4 correspond to the choice $\epsilon = 2 \times 10^{-4}$.

²⁰From Eqs. (4.7) one can verify that the elements of $\mathcal{P}_{\alpha\beta}(z)$ satisfy the following relations $\mathcal{P}_{xx}(z = \omega \pm i\eta) = \mathcal{P}_{xx}^{(1)}(\omega) \mp i\mathcal{P}_{xx}^{(2)}(\omega)$ and $\mathcal{P}_{xy}(z = \omega \pm i\eta) = \pm \mathcal{P}_{xy}^{(1)}(\omega) - i\mathcal{P}_{xy}^{(2)}(\omega)$, where $\mathcal{P}_{xx}^{(1,2)}(\omega)$ and $\mathcal{P}_{xy}^{(1,2)}(\omega)$

are real functions of the real frequency ω . We require that the effective-medium Green's function $\mathcal{G}_{\alpha\beta}^{(0)}(z)$ [and thus its self-energy $\tilde{\Sigma}_{\alpha\beta}(z)$] have the same analytical behavior for $z = \omega \pm i\eta$ as $\mathcal{P}_{\alpha\beta}(z)$.

²¹We note that we only need to solve the self-consistent problem for $z = \omega \pm i\eta$ (cf. Ref. 20).

²²In the frequency region corresponding to the impurity band, both the real and imaginary parts of the phonon self-energy show extremely rapid changes with frequency. The numerical solution of the CPA equation becomes then rather laborious, since in that case convergence is achieved only if the initial guess for the self-energy is very close to the actual root. In fact, the impurity band was missed altogether in a preliminary account of our work [A. G. Eguluz, A. A. Maradudin, and R. J. Elliott, Surf. Sci. **113**, 426 (1982)].

²³From Eqs. (5.8) and (5.9) [and the paragraph following Eq. (5.8)] we have that for $|z| \rightarrow \infty$ the self-energy $\Sigma(z) \rightarrow c + bz^{-2}$, where c is the concentration of pinning centers and b is a constant.

²⁴This result can be understood by noting that the impurity-bound state that occurs in the problem of one pinning center in an otherwise perfect lattice, is in the absence of a magnetic field, doubly degenerate. We recall that for $\nu_c = 0$ (and $\lambda = 1$), that state occurs at $\nu = 1.26$. For $\nu_c = 0.1$, the two split states occur at $\nu = 1.30$ and $\nu = 1.22$, respectively.

²⁵D. Pines, *Elementary Excitations in Solids* (Benjamin, New York, 1964), p. 34.

²⁶For comparison we note that in the experiments of Grimes and Adams (Ref. 2) the transition temperature (at which the electrons at the surface of liquid helium form a crystal) is $T_c \simeq 0.45$ K.